Environmental Engineering and Management Journal

March 2019, Vol.18, No. 3, 737-747
http://www.eemj.icpm.tuiasi.ro/; http://www.eemj.eu

"Gheorghe Asachi" Technical University of Iasi, Romania

SPOTTED GOLDEN THISTLE STALKS AS A NOVEL LOW-COST SORBENT FOR METHYLENE BLUE SORPTION FROM SYNTHETIC AQUEOUS SOLUTIONS: EQUILIBRIUM AND KINETICS STUDIES

Zoubida Senouci Bereksi, Houcine Benaïssa*

Laboratory of Sorbent materials and Water Treatment, Department of Chemistry, Faculty of Sciences, University of Tlemcen, P.O. Box 119, 13 000 Tlemcen - Algeria

Abstract

The present study explores the potential use of plant waste i.e. spotted golden thistle (*Scolymus maculatus* L.) stalks, as an inexpensive sorbent for the removal of methylene blue from synthetic aqueous solutions. Firstly, the waste material was characterized using different analysis methods, then kinetics and equilibrium of dye sorption were investigated using a batch sorption technique. The influence of contact time, initial dye concentration, sorbent dose, particle size and agitation speed on the dye sorption kinetics has been studied. The amount of dye sorbed at equilibrium increased with initial dye concentration, and with decreasing of particle size and sorbent dose. Agitation speed of 400 rpm afforded immersion of sorbent at earlier contact time and enhanced sorbed dye equilibrium amount. The necessary time to achieve equilibrium was increasing in the range of 12-19 h with initial dye concentration. Five models including first-order, pseudo second-order, Elovich, Avrami and Tobin ones were selected to describe the dye sorption kinetics. The best fitting model was the Avrami one. A multiple-stage diffusion of methylene blue onto thistle stalks particles was observed. Equilibrium data of methylene blue sorption by thistle stalks were fitted to six models namely Freundlich, Langmuir, Temkin, Sips, Toth and Redlich-Peterson models; Sips model best fitted the data. Maximum monolayer sorption capacity of sorbent was found to be 74 mg/g towards methylene blue. These first results obtained under the investigated experimental conditions, show that this sorbent is promising material for methylene blue removal from aqueous solutions.

Keywords: equilibrium, kinetics, methylene blue, sorption, spotted golden thistle

Received: January, 2016; Revised final: August, 2016; Accepted: August, 2016; Published in final edited form: March, 2019

1. Introduction

From various branches of industries using synthetic dyes to colour their products, the textile industries consume considerable amounts of water in their manufacturing processes, and, thereby generate substantial quantities of wastewater containing large amounts of dissolved dyestuffs and other products. Considering both the volume and the effluent composition, the textile industry is rated as the most polluting among all industrial sectors. Dyes colour water bodies and may hinder light penetration and photosynthetic activity and causes oxygen deficiency, thereby, affecting aquatic and vegetal life and limiting the utilization of water: it is therefore imperative to treat the textile effluents (Brown, 1987; Shertate and Prakash, 2014; Zablocka-Godlewska et al. 2015). Cationic dyes, commonly known as basic dyes, are widely used in acrylic nylon, wool and silk dyeing. This group of dyes includes a broad spectrum of different chemical structures, primarily based on the substituted aromatic groups. Due to their complex chemical structure, they are resistant to breakdown by chemical, physical and biological treatments (Eren and Afsin, 2008). Physicochemical processes including: electro-flotation, flocculation, electro-kinetic coagulation, adsorption, ion exchange, membrane filtration, precipitation, irradiation,

*Author to whom all correspondence should be addressed: e-mail: ho_benaissa@yahoo.fr

chemical destruction, ozonation etc… are generally used to treat dyes laden wastewater; however, they are costly and markedly ineffective because of the chemical stability of dyes (Forgacs et al., 2004). This situation requires the development of an eco-friendly treatment technology. Many forestry or agricultural wastes have been proposed as low cost sorbent materials for the removal of several water pollutants. The latter are ranging from heavy metals (Blázquez et al., 2018) to organic molecules such as dyes (Gunasekar et al., 2017). Agro-wastes are readily available, renewable biomass, and biodegradable, and their valorization as sorbent materials for environmental applications is an interesting alternative to costly commercial activated carbons, thus reducing any negative impact of such agro-wastes to the environment (Forgacs et al., 2004).

This study explores the possibility of using a natural plant waste material namely: spotted golden thistle (*Scolymus maculatus* L.) stalks (SML) as a novel inexpensive and abundantly available sorbent in Algeria and the Mediterranean Circum for the sorption of methylene blue (MB) from synthetic aqueous solutions. This invasive plant is often burnt or left unutilized on the fields. Literature survey reveals that use of thistle stalks as a sorbent material for the removal of hazardous dyes is an innovative initiative realized by our laboratory. MB was chosen in this study as a model dye because of its well-known strong adsorption onto solids. Historically, MB is the first synthetic compound ever used as an antiseptic in clinical therapy. From the toxicological point of view, it is relatively nontoxic and has an enviable safety record. However at very high levels, MB can be taken up by cells, accumulate and dimerize in the cytoplasmic organelles, and may cause cell toxicity and DNA damage in various cell types (Oz et al., 2009). Firstly, the raw material was characterized throughout elemental analysis, ATR – FTIR (Attenuated Total Reflectance Fourier Transform Infra-Red), specific surface area, SEM (Scanning Electron Microscopy) and SEM coupled to EDX (Electron Dispersive X ray) analysis. Then, kinetics and equilibrium studies of MB sorption were investigated in batch conditions. The effect of some operating parameters including: contact time, initial MB concentration, sorbent dose, particle size and agitation speed, on the kinetics of MB sorption from synthetic aqueous solutions by SML, was studied. The experimental data of MB sorption kinetics by this tested material were fitted by five kinetic models namely: first-order, pseudo second-order rate, Elovich (without approximation), Avrami and Tobin equations. To identify the main rate controlling steps in the overall uptake mechanism, external and intra-particle diffusion models were separately examined for each operating sorption parameter studied. The experimental data of dye sorption equilibrium were fitted to three 2-parameters isotherm models: Freundlich, Langmuir and Temkin, and, to three 3-parameters isotherm models: Sips, Toth and Redlich-Peterson models. In this work, the kinetic and equilibrium models were fitted employing the non-linear regression method. Therefore, this work could provide useful information for the utilization of SML as an innovative sorbent for the removal of cationic dyes.

2. Material and methods

2.1. Sorbent and dye

A natural plant waste material namely: Spotted golden thistle (*Scolymus maculatus* L.) stalks, was used as a sorbent material in this work. This waste was collected from the region of Bensekrane (Tlemcen - Algeria) in autumn-winter period 2010 in the form of dried large flakes. It was cut manually in small pieces (1−2 cm) with a pruning shears and gently washed with tap water, then oven-dried at (85 ± 5)°C for 24 h. Prior to be used as a sorbent material, this waste was washed thoroughly with distilled water until constant pH and no leaching of colour were observed. Thereafter the material was filtered, then oven-dried for another time at (85 ± 5)°C for 24 h to a constant weight. Then, it was crushed and sieved to keep only the size range of 0,630−2 mm, and immediately stored in desiccators.

Methylene blue as a commercial salt (REACTIF RAL -France), was used as received without further purification. 1000 mg/L stock solutions of this dye were prepared in distilled water. All working solutions of desired concentration were prepared by accurate dilutions.

2.2. Sorbent characterization

The sorbent was characterized using different analytical techniques:

- The sorbent percentage contents of C, H, N and O were determined using a homemade elemental analyser, while the S percentage content was obtained thanks to (LECO SC 144) system (Solaize Central Service of Analysis -University of Claude Bernard Lyon I France).

- ATR (attenuated total reflectance) technique allows the direct IR analysis of solid samples without any impact from the traditional KBr pellet sampling: Spectra of MB, SML, and dye loaded sorbent (MB-SML) samples, were recorded with a Perkin Elmer Spectrum 100-FTIR equipped with a Zn-Se crystal, in the 4000−600 cm^{-1} range (resolution = 4 cm^{-1} , 10−20 cumulative scans).

- The BET surface area of SML was obtained from liquefied N_2 adsorption isotherm at 77 K, using a Micromeritics Flowsorb II 2300 surface area analyser. Prior to the adsorption experiments, the sample was degassed at 125 °C in vacuum for 48 h.

- The surface morphology of both SML and MB-SML was examined by scanning electron microscopy (SEM), using a Jeol JSM 6301 F microscope. Furthermore the SEM coupled to the electron dispersive X-ray (SEM-EDX) microanalysis method, was performed using Jeol JSM 6400

equipped of Oxford INCA treatment software. All samples were coated with a thin layer (80 % gold, 20 % platinum) prior to the observations.

2.3. Sorption experiments

2.3.1. Uptake kinetics

For all experiments 1 g (except for sorbent dose effect) of sorbent was added to a beaker containing 1 L of MB solution, which initial concentration was 100 mg/L (except for initial MB concentration effect). A magnetic stirrer allowed agitation (mandatory at earlier stages of contact between sorbate and sorbent used) at 400 rpm (except for agitation speed effect). A water bath maintained a constant temperature of (25 ± 1) °C. Particle size of the sorbent was in the range of 0.630–2 mm (except for particle size effect). Initial pH of MB solutions was in the range of 3.1−4.8 and was not adjusted. Samples from the clear supernatant were withdrawn at appropriate time intervals, and their dye concentrations were determined using UV-Vis spectrophotometer (HACH LANGE DR 5000) at λ_{max} = 664 nm.

The dye uptake [q_t (mg/g)] was calculated with (Eq. 1):

$$q_t = \frac{(C_0 - C_t)V}{m} \quad (1)$$

where C_0 and C_t are the initial concentration (mg/L) and the concentration (mg/L) at time t (h), respectively; V is the volume of solution (L) and m denotes the mass of the dry sorbent (g). Duplicate if not triplicate, tests showed that the maximum standard deviation of the results was ± 7 %.

2.3.2. Uptake equilibrium

MB sorption isotherm was determined using a series of 250 mL conical flasks by contacting a constant mass of 0.250 g of the sorbent material with 0.250 L of MB solution of different initial concentrations (20−700 mg/L). This range was judged sufficient to enable the overall shape of the isotherm to be determined. After a period of 30 h at (25 ± 1) °C, the equilibrium concentrations [C_e (mg/L)] of unbound MB were determined with visible spectrophotometry, as described previously in the case of C_t; and the corresponding equilibrium MB uptakes [q_e (mg/g)], were obtained with (Eq. 1); taking into account that q_t and C_t becomes q_e and C_e respectively, when the sorption equilibrium is achieved. Initial as well as final solutions pH values were also measured.

3. Results and discussion

3.1. Sorbent characterization

3.1.1. Characteristics before MB sorption

The elemental composition of SML was: C 44.42 %, O 42.81 %, H 5.97 %, N < 0.30 % and S < 0.30%, indicating that the sorbent material is rich in carbon and oxygen, as normally expected for lignocellulosic materials, but contains almost nil level of sulphur.

ATR-MIR spectrum (Fig. 1) of SML permits to check the presence of:

- ***Holocellulose***: thanks to four polysaccharides characteristic bands between 1200 and 1000 cm^{-1}. The glycosidic linkage is largely responsible of the higher frequency band (1156 cm^{-1}) in this region, the other bands are at 1105, 1050 and the more intense band is at 1029 cm^{-1}. Polysaccharides presence is enhanced by the band at 897 cm^{-1} as β-anomer vibration (Kacurakova et al., 2000). Bands at 1423, 1371, 1325 and 1206 (shoulder) cm^{-1} are respectively significant of CH_2 bending, OH bending, skeletal (C−C and C−O) vibrations (Sun et al. 2004), and pyranose ring C−O stretching (Pastorova et al., 1994). Among this holocellulose content there are some hemicelluloses: According to latest works (Célino, et al., 2014) dealing with ATR-FTIR studies on vegetal fibres, hemicellulose gives bands at 1735 cm^{-1} (C=O) and 1240 cm^{-1} (C−O, acids or esters). Abidi, et al., (2014) showed that the band assigned to ester at 1735 cm^{-1} due to hemicelluloses is decreasing with fibre developmental time, and getting very small intensity on maturation. In case of SML these 2 bands are located at 1734 (small) and 1236 cm^{-1}. Also simultaneous presence of bands at 1734, 1596 and 1423 cm^{-1} is significant of carboxylic functions of hemicelluloses (Marchessault, 1962).
- ***Lignin:*** The large band at ~1596 cm^{-1} is common to hemicelluloses and lignin vibrations. When lignin is present, a second band is observable at 1505 cm^{-1} (Kacurakova et al., 2000), the intensity of which is similar or higher (Vazquez et al., 1997). So, in the present case of SML, conclusion is made that low amounts of lignin are accompanying hemicelluloses, due to lower intensity at 1505 cm^{-1} than at 1596 cm^{-1}. Similarly to the present work, Célino et al., 2014 reported the presence of low amounts of lignin, on the basis of ATR-FTIR spectra on vegetal fibres directly, without previous extraction.
- ***Water*** is also present at given amount due to broadening around 1650 cm^{-1}, of the band at 1596 cm^{-1} (Olsson et al., 2004).

The BET surface area of the sorbent was found to be 1.66 m^2/g. This low value of surface area is characteristic of biomass materials (Pavan et al., 2014).

The SEM micrographs of the sorbent before MB sorption (Figs. 2a,b), show different morphologies depending on the region analysed, and, a rough surface with crater-like cavities with macro-porous structures, as a general. These cavities are large enough to allow the molecules of dye to penetrate into the lignocellulosic structure and interact therein with the surface groups. Fig. 2a also reveals the fibrous structure of SML with a network of organized fibres.

3.1.2. After MB sorption

MB-SML Spectrum (Fig. 1) is not the simple addition of each SML and MB spectra (Fig. 1), taken

as alone: it is the spectrum resulting from interactions between each other.

Therefore, two comparisons must be done: MB-SML spectrum with MB one alone, as well as MB-SML spectrum with SML one alone. These comparisons, needs the prior examination of MB spectrum, which shows an immense and flattened in shape band in the region 3600−2500 cm^{-1}; with several small emergences. According to Ovchinnikov et al., (2007), those at ~3070 and ~3030 cm^{-1} are due to heterocyclic CH stretching, that at ~ 2817 cm^{-1} is due to $-N(CH_3)_2$ vibrations and the one at ~2706 cm^{-1} is due to water hydrogen bonds with the MB nitrogen atoms (O−H-N). For some bands lying under 1800 cm^{-1}, assignments are summarized in Table 1.

a. Comparing MB-SML spectrum with MB spectrum allows the following statements:

- The little band at 1653 cm^{-1} (immonium vibration) gets higher intensity after sorption and makes distinguished shoulder on the broad band at 1596 cm^{-1}. This shoulder is likely being due to immonium contribution than to increased amount of water, since SML and MB-SML have been dried to the same extent.

- Band at 2706 cm^{-1} due to hydrogen bonds (O-H--N) is significant of either direct interaction between OH groups (holocellulose + lignin) at SML surface and MB nitrogen atoms, and/or indirect interaction between water OH groups and MB nitrogen atoms; this indirect interaction means intercalated water molecules between SML surface and MB sorbed in accordance of proposals from Ovchinnikov et al., (2007). Thereafter more contribution of immonium vibration -meaning more delocalized global positive charge towards external amines groups- is likely occurring as well as intercalated water molecules.

- Although not explained other modifications are relevant of interaction between MB and SML: Disappearance of both bands at 1544 cm^{-1} and at 1280 cm^{-1}.

b. Comparison between MB-SML and SML spectra, leads to observe shifts of 17 and 11 cm^{-1} respective to bands at 1371 and 1320 cm^{-1}. Even if higher than the resolution of spectrophotometer used, these shifts are not significant since they overlap bands from MB (1388 and 1331 cm^{-1}). On contrary the shoulder at 1206 cm^{-1} is absent after sorption, due to shift to higher frequencies of the C−O (pyranoses rings) stretching vibrations. At the opposite glycosidic γ(C−O−C) vibration band shifts from 1156 to 1143 cm^{-1} (e.g. -13 cm^{-1}).

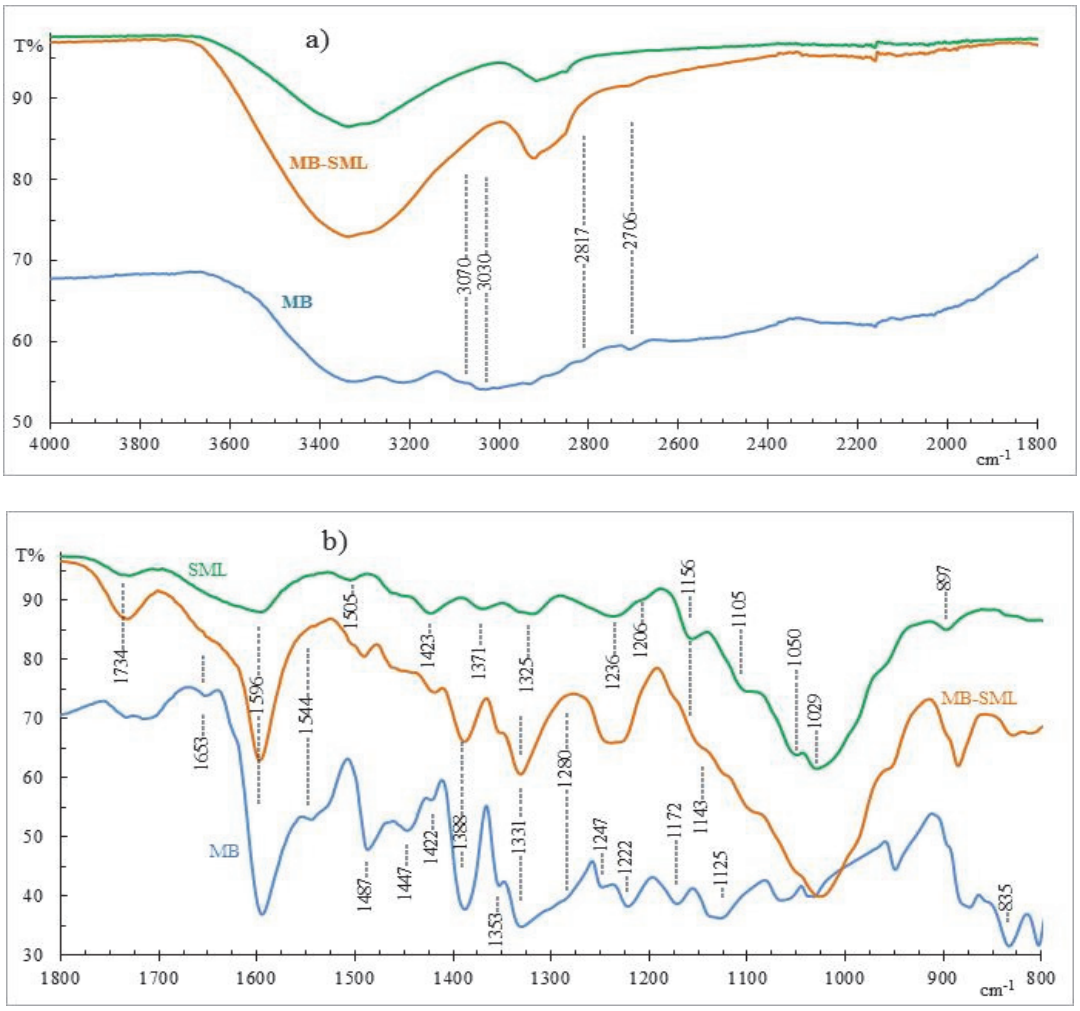

Fig. 1. ATR-FTIR spectra of SML, MB and MB-SML: a) In the wavenumber range of 4000−1800 cm^{-1}, b) in the wavenumber range of 1800−800 cm^{-1}

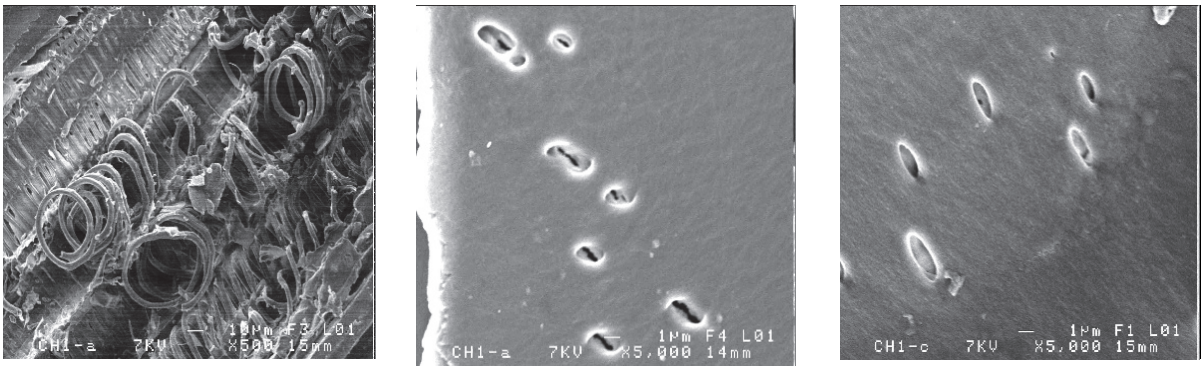

(a) (b) (c)

Fig. 2. SEM micrographs of SML: (a, b) before MB sorption (500 x and 5000 x, respectively) and (c) after MB sorption (C_0= 100 mg/L, t_{eq} over 19 h, m= 1 g/L, d_p= 0.630−2 mm, natural solution pH, T= 25 °C) (5000 x)

Table 1. Assignments of some ATR-MIR MB bands

Bands (cm^{-1})	*Assignments*	*References*	*Bands (cm^{-1})*	*Assignments*	*References*
1653	$=N^+$	Ovchinnikov et al., 2007	1247	$N-CH_3$	Xu et al., 2011
1595	Skeletal heterocyclic vibrations	Ovchinnikov et al., 2007; Vargas et al., 2011	1222	Aromatic skeletal vibrations	Ovchinnikov et al., 2007
1487			1172	$N-CH_3$	Xu etal., 2011
1447	$C-H_3$ and C−C (aromatic)	Ovchinnikov et al., 2007	884–873	Heterocyclic CH bending	Vargas et al., 2011
1388	Multiple ring stretching	Xu et al., 2011	835		
1331	$C_{ar}-N$				

Hence MB sorption leads to opposite effects on (C−O) bonds within and between pyranoses rings. Glycosidic linkage is weakened after sorption, due to higher electronic density in pyranoses rings. On the one hand increased pyranoses rings electronic density helps better interaction with positive moieties of intercalated water molecules (involved through negative moieties, in interaction with MB cations), and on the other hand, is extended to attached OH groups which are involved in direct interaction with MB.

All these findings support the existence of strong electrostatic interactions between the MB cation, (which charge is more delocalized after sorption) and the partial negative charges at surface of SML; these being due at least to hydroxyl groups from holocellulose and or lignin. These interactions involve also intercalated water molecules.

- The SEM micrograph of MB-SML (Fig. 2c), shows a rough surface with narrowed crater-like pores because they are partially covered by the MB dye, so that the pores are seen more blurred than in the sample before dye sorption. The ability of sorbent to remove MB was evidently confirmed by the visual observation of sorbent colour after dye sorption experiments. However, it should be interesting to point out that the results of dispersive X-ray (EDX) analysis of SML, showed an absence of sulphur at anyway targeted position of SML sample surface. On the contrary, SML-MB EDX showed adequate level of sulphur at any targeted surface point, due to uniform coverage by the dye.

3.2. Sorption kinetics

3.2.1. Effect of contact time and initial dye concentration

The contact time is one of the most important operating parameters in the sorption process. Its effect on the sorption of MB by thistle stalks is illustrated on Fig. 3. This figure deals with the typical example of initial MB concentration of 100 mg/L, and shows that the sorption kinetics curve obtained is characterized by a strong increase of the amount of MB sorbed during the initial stage of contact, followed by a gradual increase until to reach a state of equilibrium. The equilibrium amount of MB sorbed being q_e = 37 mg/g and the necessary time t_{eq} to reach this equilibrium is around 19 h. An increase of sorption contact time up to 30 h did not show any notable effect. Increasing initial MB concentrations (50, 80, 100 and 150 mg/L) was followed up by an increase of equilibrium amount of MB sorbed (22, 34, 37 and 55 mg/g). This trend was expected since the initial MB concentration provides an important driving force to overcome all mass transfer resistances of the dye between the aqueous and solid phases. MB sorption kinetics was slow, achieving equilibrium around 12 h (C_0= 50 mg/L), 17 h (C_0= 80 mg/L) and 19 h (C_0=100 and 150 mg/L).

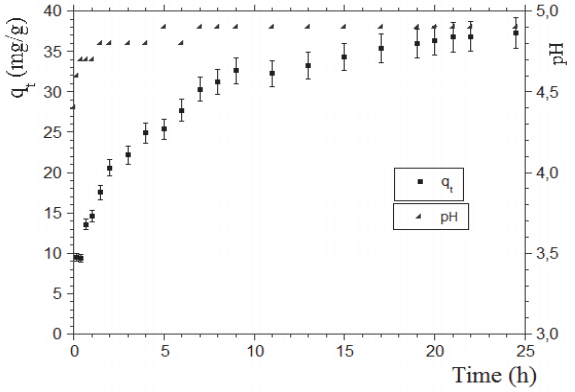

Fig. 3. Kinetics of MB (C_0 = 100 mg/L) sorption from aqueous solution by SML (1g/L) $q_t = f(t)$ and pH = f (t)

During the course of MB sorption by the tested sorbent SML, an increase in the solution pH value of the solution followed by some equilibrium states was observed; the double y axis graph of Fig. 3 gives an illustration of this behaviour, for the initial MB concentration of 100 mg/L. Such increase of the pH values suggests that MB binding to SML is either associated with the fixation -of H_3O^+ ions from solution by the sorbent surface -or with a release of OH^- ions from the sorbent surface into the solution. This trend was also observed for all other operating parameters studied thereafter.

3.2.2. Effect of sorbent dose

In order to determine the minimal SML dose for optimal sorption of MB, kinetic studies were performed using different sorbent doses (0.5−4 g/L). Fig. 4 shows that q_e, the equilibrium amount of methylene blue sorbed by thistle stalks, increases from 30 to 37 mg/L with increase of the sorbent dose m, from 0.5 to 1 g/L; when sorbent dose is further increased up to 2 g/L q_e remains nearly constant. However any augmentation beyond 2 g/L leads to a decline of sorption. The enhancement of q_e due to increase of m from 0.5 to 1 g/L was expected since more sorption sites are being available for solute-sorbent interaction; nevertheless more significant increase of m may results in some particles aggregation leading to a decrease in the total surface area of sorbent and an increase in the diffusional path length (Ofomaja and Ho, 2007); thereby resulting in the decreased dye uptake. Thus, SML dose of 1 g/L was further chosen for all remaining studies. This low dose affords more convenience during withdrawing of samples, avoiding sorbent particles to be sucked up in the pipette.

3.2.3. Effect of agitation speed

In the goal to study the impact of agitation on the sorption kinetics of MB by SML, different agitation speeds: 200, 400, 500 and 600 rpm were tested. Agitation afforded immersion of the sorbent particles which otherwise had floated to the surface. Agitation was mainly maintained during the earlier contact period and could be interrupted beyond one hour -when all sorbent particles were immersed (the batches being stirred from time to time with the thermometer).

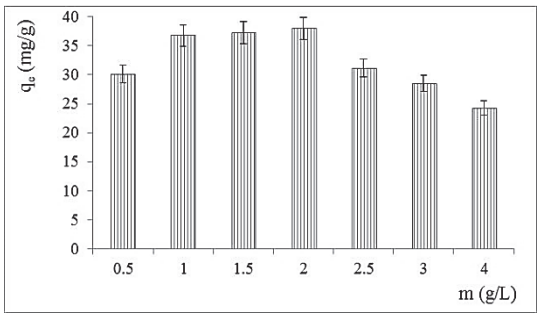

Fig. 4. Effect of sorbent dose on MB equilibrium uptake by SML (C_0 = 100 mg/L, t_{eq} ~19 h, d_p= 0.630−2 mm, natural solution pH, T = 25 °C)

Fig. 5 shows that 400 rpm is optimal agitation speed. It was chosen for all the remaining experiments since it assures at earlier stages of contact a good diffusion of dye toward SML particles avoiding flotation of SML which may screen the active binding sites, as well as an insufficient time to bind with dye cations (Hossain et al. 2012).

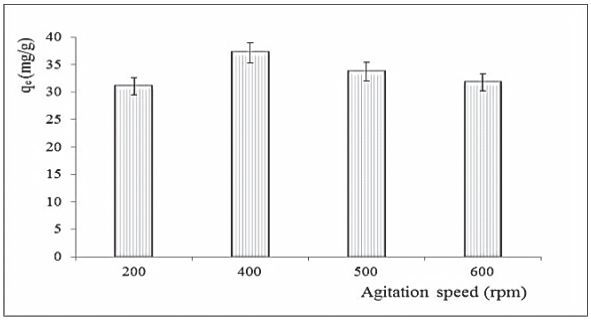

Fig. 5. Effect of 1h-agitation on MB equilibrium uptake by SML (C_0 = 100 mg/L, m= 1g/L, d_p= 0.630−2 mm, natural solution pH, T= 25 °C)

3.2.4. Effect of particle size

To study the effect of particle size d_p on MB sorption kinetics by SML, experiments were conducted with six particle size ranges: $0.63 < d_p \leq 1.25$ mm; $1.25 < d_p \leq 1.6$ mm; $1.6 < d_p \leq 2.0$ mm; $2.0 < d_p \leq 2.5$ mm; $2.5 < d_p \leq 3.15$ mm and $d_p > 3.15$ mm. Fig. 6 indicates that the amount of dye sorbed by SML at equilibrium, q_e, increases in general by decreasing the particle sizes of sorbent: 22 mg/g (dp > 3.15 mm) to 36 mg/g (0.63 < dp < 1.25 mm).

This behaviour can be attributed to an increase of effective surface area of the sorbent with the decrease of particle size; consequently, the dye sorption increases (Hossain et al., 2012). However, moderate if not negligible increase of q_e values is obtained for particle sizes in the global range of 0.630−2 mm, suggesting MB sorption to occur at less external surface. This assumption is supported by the astonishing helical spring like structures shown by SEM micrographs (Fig. 2a).

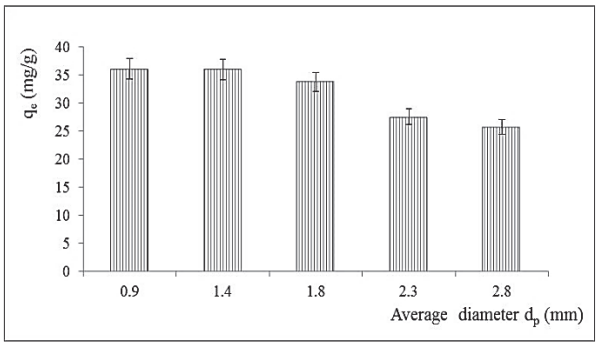

Fig. 6. Effect of particle average diameter on MB equilibrium uptake by SML (C_0 = 100 mg/L, t_{eq} ~19 h, m = 1 g/L, natural solution pH, T = 25 °C)

3.2.5. Kinetics modelling

In order to describe the kinetics of MB sorption by SML obtained at different experimental conditions, five kinetic models namely: first-order model (Lagergren, 1898), pseudo second-order model (Ho and McKay, 1998), Elovich model (Low, 1960), Avrami model (1940) and Tobin model (1974) in their non-linear forms, have been used. The non-linearized forms of these models are given in Table 2.

In this work, the above mentioned kinetic models were fitted using the nonlinear regression method (Excel 2007 software); high value of the correlation coefficient R^2 being obtained for satisfactory fit. The calculated kinetic parameters and corresponding R^2 values are listed in Table 3; effect of initial concentration being a typical example.

Table 3 shows that the Avrami fractionary order, Elovich, Tobin and pseudo second-order kinetic models, in decreasing ranking were suitably fitted; whereas Lagergren model failed with lowest R^2 value. This general ranking was also observed with all kinetics for each operating parameters studied (Tables of results not shown in this work). Except for Elovich model, which is not belt on consideration of desorption and hence on equilibrium achievement (Rudzinski and Plazinski, 2009), all the suitably fitted models gave values of the calculated equilibrium amounts of MB sorbed ($q_{e\,cal}$); this theoretical values were in good agreement with the experimental ones ($q_{e\,exp}$), whatever the experimental parameter studied. Taking into account that, in the above mentioned general ranking of models there are 2-parameters models and less affordable 3-parameters models, it makes sense to prefer the Elovich one. Based on this satisfactory fitting model and calculating the approaching equilibrium factor R_E which is $(q_e\beta)^{-1}$ (Wu et al., 2009), led to values between 0.18 and 0.23. Thus, conclusion is made that all the kinetic curves of MB sorption on SML are of mild rising type, since obtained R_E obey to $0.3 > R_E > 0.1$.

3.2.6. Rate determining steps

Sorption is a process involving several elementary steps. Generally, the two rate limiting steps investigated are external film mass transfer and intraparticle diffusion, either singly or in combination.

a) External mass transfer resistance model: The initial rate of sorption can be determined using the (Eq. 2) (McKay and Poots, 1984):

$$\left(\frac{d(C_t/C_0)}{dt}\right)_{t\to 0} = -\beta_L S \qquad (2)$$

In (Eq. 2) β_L and S are respectively, the external mass transfer coefficient and the specific surface area of the sorbent. The external mass transfer rate, $\beta_L S$, is approximated by the initial slope of the C_t/C_0 *vs.* time curve; assuming a polynomial relation.

b) Intraparticle diffusion resistance model**:** Weber and Morris (1963) demonstrated that in intraparticle diffusion studies, process rate**s** are usually expressed in terms of square root of time, with (Eq. 3):

$$q_t = k_{id} t^{1/2} \qquad (3)$$

where k_{id} is defined as an intraparticle diffusion rate parameter. It is obtained as the slope of the plot of q_t *vs.* $t^{1/2}$. This plot should be linear if intraparticle diffusion is involved in the sorption process; moreover, if passing through the origin, then intraparticle diffusion is the rate controlling step.

In the present work the two kinds of transfer resistance were separately tested and results are summarized in Table 4. Fitting experimental data (related to each operating parameter studied) to intraparticle diffusion model led to multi linear plots which clearly confirm that the process involves more than one kinetic stage before achieving the equilibrium. Positive and generally significant ordinate intercepts obtained reflects some degree of boundary layer control at earlier contact time, in accordance of results from external diffusion model; therefore, intraparticle diffusion is not the fully operative mechanism for this system.

3.3. Sorption equilibrium

3.3.1. Sorption isotherm

As shown in Fig. 7, the experimental isotherm of methylene blue sorption by thistle stalks at natural solution initial pH (3.1–4.8) and 25 °C shows a rapid increase of q_e for low C_e values, followed by a moderate increase until a saturation plateau is reached. Thus it may be rated as L-type, according to the classification of Giles et al. (1960) for liquid-solid adsorption.

The maximum capacity of MB sorbed by this sorbent, q_{max}, is about 65 mg/g under the experimental conditions being tested in this work. However at higher C_e, some decline in the sorption of MB was observed (not shown on Fig. 7): Such findings were pointed out by other authors (Samiey and Dargahi, 2010). As previously mentioned in kinetic studies, an increase in the solution pH value was again observed before contact with SML and after sorption equilibrium was achieved (final pH in the range of 4.1–5.4).

Table 2. Mathematical equations of kinetic models tested for MB sorption by SML

Models	***Expressions***	***Parameters***
First order	$q_t = q_e(1 - e^{-k_f t})$	q_e : Equilibrium MB uptake (calculated)
		k_f: Pseudo first-order model rate constant
Pseudo second-order	$q_t = \frac{k_s q_e^2 t}{1 + k_s q_e t}$	q_e : Equilibrium MB uptake (calculated)
		k_s: Pseudo second-order model rate constant
Elovich	$q_t = \beta^{-1}\ln(1 + \alpha\beta t)$	α: Initial rate of Elovich model
		β: Elovich model constant
Avrami	$q_t = q_e(1 - e^{-(k_A t)^{n_A}})$	q_e : Equilibrium MB uptake (calculated)
		k_A: Avrami model rate
		n_A : Avrami exponent
Tobin	$q_t = \frac{q_e k_T t^{n_T}}{1 + k_T t^{n_T}}$	q_e: Equilibrium MB uptake (calculated)
		k_T: Tobin model rate
		n_T : Tobin exponent

Table 3. Parameters and R^2 values of kinetic models tested for MB sorption by SML

Models	***C_0 (mg/L)***	***50***	***80***	***100***	***150***
	$q_{e\,exp}$ (mg/g)	21.8	33.6	37.2	55.5
First-order model	$q_{e\,cal}$ (mg/g)	20.3	32.4	34.7	50.4
	k_f (h^{-1})	0.36	0.29	0.39	0.38
	R^2	0.9392	0.9685	0.9226	0.9386
Pseudo second-order model	$q_{e\,cal}$ (mg/g)	21.4	34.4	38.6	56.6
	k_s ($mg^{-1}.g.\ h^{-1}$)	0.027	0.014	0.015	0.009
	R^2	0.9698	0.9739	0.9687	0.9818
Elovich model	α ($mg.\ g^{-1}.h^{-1}$)	26.59	29.08	60.47	63.29
	β ($mg^{-1}.\ g$)	0.23	0.13	0.14	0.09
	R^2	0.9853	0.9808	0.9897	0.9950
Avrami model	$q_{e\,cal}$ (mg/g)	21.2	34.7	37.7	54.9
	k_A (h^{-1})	0.32	0.24	0.31	0.30
	R^2	0.665	0.684	0.574	0.633
		0.9875	0.9891	0.9901	0.9956
Tobin model	$q_{e\,cal}$ (mg/g)	21.4	34.8	38.3	55.2
	k_T (h^{-n_T})	0.60	0.42	0.66	0.60
	n_T	0.970	1.082	0.887	0.930
	R^2	0.9699	0.9784	0.9735	0.9816

Table 4. Effect of various experimental parameters on diffusion coefficients for MB sorption by SML

	External diffusion		***Internal diffusion***		
	$\beta_L S$ (h^{-1})	***R^2***	***Intercept (mg/g)***	***k_{id} ($mg.g^{-1}.h^{-1/2}$)***	***R^2***
Co (mg/L)					
50	0.36	0.9920	1.4	6.19	0.9860
80	0.27	0.9927	0.4	10.31	0.9946
100	0.33	0.9736	13.7	5.32	0.9862
150	0.29	0.9955	23.2	7.50	0.9784
d_p (mm)					
> 3.15	0.19	0.9870	3.0	4.49	0.9898
3.15-2.5	0.24	0.9824	6.1	4.76	0.9833
2.5-2.0	0.28	0.9906	4.1	5.56	0.9925
2.0-1.6	0.35	0.9694	11.0	5.18	0.9967
1.6-1.25	0.45	0.9700	14.3	5.17	0.9833
1.25-0.63	0.46	0.9610	15.0	5.13	0.9646
m (g/L)					
0.5	0.15	0.9957	10.3	4.72	0.9754
1	0.33	0.9736	13.7	5.32	0.9862
1.5	0.43	0.9905	15.8	4.92	0.9959
2	0.73	0.9877	14.3	5.61	0.9867
2.5	0.80	0.9943	17.2	3.23	0.9936

3	1.04	0.9898	14.4	4.06	0.9951
4	1.20	0.9845	14.3	2.82	0.9808
N (rpm)					
200	0.24	0.9910	8.3	5.48	0.9628
400	0.33	0.9736	13.7	5.32	0.9862
500	0.25	0.9935	9.2	5.99	0.9634
600	0.30	0.9902	10.3	4.99	0.9886

In order to situate the sorbent -being investigated for the first time- among those used (without preliminary chemical modification) to remove MB from aqueous solutions, a comparison based on the q_{max} values from literature, was carried out and is presented on Table 5.

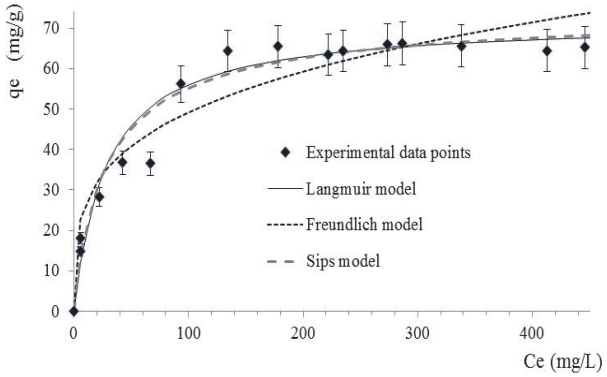

Fig. 7. Sorption isotherm of MB on SML at T = 25 °C: experimental points and calculated curves.

Lignocellulosic materials selected for this comparison are largely and easily available; in addition preliminary treatments before use as sorbents do not necessitate neither huge volumes of water, nor significant levels of energy expenditure. In addition, the overall studies reported on Table 5 give q_{max} values which are clearly experimentally verified.

Being mindful of the varying experimental conditions during the investigations of the sorbent materials reported on Table 5, it can be however stated that thistle stalks, as reclaimed waste, are promising low cost sorbent**s** for discolouring water, due to significant sorption capacity.

3.3.2. Isotherm modelling

To describe the isotherm of MB sorption by SML obtained under the above mentioned experimental conditions, six models were used: Freundlich (1906), Langmuir (1916), Temkin (1941), Redlich-Peterson (1959), Sips (1948) and Toth (1981).

Table 5. Comparison of maximum MB sorption capacities of various waste materials from literature

Sorbents	***d_p (mm)***	***m(g/L)***	***pH_0***	***t_{eq} (h)***	***T(°C)***	***q_{max}(mg/g)***	***References***
Brazil nut shells	0.5-0.71	100	6.5	2	-	8	Brito et al., (2010)
Wood shavings	3-4	20	5.5	< 72	-	19	Janos et al., (2009)
Rice husk	0.60 – 0.85	1.2	8	2	32	41	Vadivelan and Kumar, (2005)
Thistle stalks	0.630-2	1	3.1-4.8	≤ 19	25	65	This work
Hazelnut shells	0.075-0.180	10	-	1	20	77	Ferrero, (2007)
Sesame straw	≤ 0.250	1	8	-	25	170	Feng et al., (2017)
Guava leaf	0.10-0.15	2	7.5	≤ 3	30	295	Ponnusami et al., (2008)

Table 6. Mathematical equations of equilibrium models tested for MB sorption by SML

Models	***Expressions***	***Parameters***
Freundlich	$q_e = K_F C_e^{n_F}$	K_F : Freundlich sorption isotherm constant
		n_F : Freundlich exponent
Langmuir	$q_e = \frac{q_{max} K_L C_e}{1 + K_L C_e}$	q_{max} : Maximum equilibrium sorbed amount of dye on unit mass of sorbent (calculated)
		K_L: Langmuir sorption isotherm constant
Temkin	$q_e = B_{Tm} \ln(A_{Tm} C_e)$	A_{Tm} and B_{Tm}: Temkin sorption isotherm constants
Redlich-Peterson	$q_e = \frac{A_{RP} C_e}{1 + K_{RP} C_e^{n_{RP}}}$	A_{RP} and K_{RP}: Redlich-Peterson sorption isotherm constants
		n_{RP} : Redlich-Peterson exponent
Sips	$q_e = \frac{q_{max} K_S C_e^{n_S}}{1 + K_S C_e^{n_S}}$	q_{max}: Maximum equilibrium sorbed amount of dye on unit mass of sorbent (calculated)
		K_S: Sips sorption isotherm constant
		n_S : Sips exponent
Toth	$q_e = \frac{q_{max} C_e}{\left(B_{Th} + C_e^{n_{Th}}\right)^{1/n_{Th}}}$	q_{max}: Maximum equilibrium sorbed amount of dye on unit mass of sorbent (calculated)
		B_{Th}: Toth sorption isotherm constant
		n_{Th} : Toth exponent

Table 7. Parameters and R^2 values of isotherm models for MB sorption by SML at 25 °C

Langmuir model	***R^2 = 0.9804***	***Sips model***	***R^2 = 0.9814***	
$q_{max\ cal} = 71.9\ mg.g^{-1}$	$K_L = 0.035\ L.mg^{-1}$	$q_{max\ cal} = 74.4\ mg.g^{-1}$	$K_S = 0.05(mg^{-1}.L)^{n_S}$	n_S = 0.892
Freundlich model	***R^2 = 0.9320***	***Redlich-Peterson model***	***R^2 = 0.9811***	
$K_F = 14.20\ mg.g^{-1}.(mg^{-1}.L)^{n_F}$	n_F = 0.270	$A_{RP} = 2.17\ L.g^{-1}$	$K_{RP} = 0.02\ (mg^{-1}.L)^{n_{RP}}$	n_{RP} =1.054
Temkin model	***R^2 = 0.9479***	***Toth model***	***R^2 = 0.9806***	
A_{Tm} = 0.63 $L.mg^{-1}$	B_{Tm} = 12.6 $mg.g^{-1}$	$q_{max\ cal} = 73.6\ mg.g^{-1}$	$B_{Th} = 18.57\ (mg.L^{-1})^{n_{Th}}$	n_{Th} = 0.903

The non-linearized forms of these models are given in Table 6. In this work experimental data were fitted to these theoretical isotherms, using non-linear regression method (Excel 2007 software); R^2 value being assessment parameter for the fit. Table 7 summarizes the calculated constants for each model and the related R^2 values obtained. Table 7 shows that Langmuir model and the three 3-parameters models e.g. Sips, Redlich-Peterson and Toth models, describe suitably the experimental isotherm. Their fitting curves are all nearly confounded: For reason of clarity, Langmuir and Sips models curves are the alone ones drawn on the graph of Fig. 7. This graph contains also the curve of the worst fitting model e.g. the Freundlich model. Such applicability of theoretical models is to be considered as a mathematical representation of the dye sorption: the good fit alone, must not lead to mechanistic conclusions.

4. Conclusions

This study has demonstrated that the use of thistle stalks as a sorbent material for methylene blue removal from synthetic aqueous solutions is feasible under the experimental conditions tested in this work. Results from batch experiments showed that the amount of MB sorbed by SML at equilibrium increased with initial dye concentration, and, with decreasing of particle size and sorbent dose. MB sorption kinetics was slow and the necessary time to achieve equilibrium was initial dye concentration dependent. To describe the MB sorption kinetics, the best fitting model was the Avrami model followed by Elovich, Tobin and pseudo second-order models, respectively. Intraparticle diffusion was not a fully operative mechanism for this system. The MB sorption equilibrium by SML was suitably fitted to Langmuir, Sips, Redlich-Peterson and Toth models. Maximum monolayer sorption capacity of sorbent was deduced from Sips model and was found to be 74 mg/g at natural solution pH and 25 °C.

The obtained results are quite encouraging but there are still several major aspects to clarify in order to use this sorbent as an alternative clean-up material for contaminated wastewaters.

Acknowledgements

This work has been supported by Ministry of High Education and Scientific Research, Algeria (Project N°: J01020200110020). The authors express their sincere gratitude to Professor B. Tabti Dean of Sciences Faculty – University of Tlemcen, for material assistance. Professors A. Amrane, A. Szymczyk, M. Rabiller-Baudry and O. Merdrignac-Conanec from UMR CNRS 6226 of Rennes 1 University -France, are acknowledged for MEB/EDS, ATR-FTIR and Specific surface measurements respectively. Pr. M. Bouazza from Faculty of Biology - Tlemcen University is acknowledged for naming the plant.

References

Abidi N., Cabrales L., Haigler C.H., (2014), Changes in the cell wall and cellulose content of developing cotton fibers investigated by FTIR spectroscopy, *Carbohydrate Polymers*, **100**, 9-16.

Avrami M., (1940), Kinetics of phase change. II Transformation-time relations for random distribution of nuclei, *Journal of Chemical Physics*, **8**, 212-224.

Blázquez G., Calero M., Trujillo C., Martín-Lara Á., Ronda A., (2018), Binary biosorption of Cu(II)-Pb(II) mixtures onto pine nuts shell in batch and packed bed systems, *Environmental Engineering and Management Journal*, **17**, 1349-1361.

Brown D., (1987), Effects of colorants in the aquatic environment, *Ecotoxicology Environment Safety*, **13**, 139-147.

Célino A., Goçalves O., Jacquemin F., Fréour S., (2014), Qualitative and quantitative assessment of water sorption in natural fibers using ATR-FTIR spectroscopy, *Carbohydrate Polymers*, **101**, 163-170.

Eren E., Afsin B., (2008), Investigation of a basic dye adsorption from aqueous solution onto raw and pre-treated bentonite surfaces, *Dyes and Pigments*, **76,** 220-225.

Feng Y., Liu Y., Xue L., Sun H., Guo Z., Zhang Y., Yang L., (2017), Carboxylic acid functionalized sesame straw: A sustainable cost-effective bioadsorbent with superior dye adsorption capacity, *Bioresource Technology*, **238,** 675-683.

Ferrero F., (2007), Dye removal by low cost adsorbents: Hazelnut shells in comparison with wood sawdust, *Journal of Hazardous Materials*, **142**, 144-152.

Forgacs E., Cserhati T., Oros G. (2004), Removal of synthetic dyes from wastewater: a review, *Environment International*, **30**, 953-971.

Freundlich H.M.F., (1906), Over the adsorption in solution, *Journal of Physical Chemistry*, **57A**, 385-470.

Giles C.H., Mac Ewan T.H., Nakhwa S.N., Smith D.J., (1960), Studies in adsorption: A system of classification of solution adsorption isotherms and its use in diagnosis of adsorption mechanisms and measurements of specific areas of solids, *Chemical Society*, **14**, 3973-3993.

Gunasekar V., Ramadoss G., Ponnusami V., (2017), Influence of process variables on adsorption of Congo red onto mango leaf char using factorial design analysis, *Environmental Engineering and Management Journal*, **16**, 2745-2753.

Ho Y-S., McKay G., (1998), The kinetics of sorption of basic dyes from aqueous solution by sphagnum moss peat, *Canadian Journal of Chemical Engineering*, **76**, 822-827.

Hossain M.A., Ngo H., Guo H.W.S., Nguyen T.V., (2012), Removal of copper from water by adsorption onto banana peel as bioadsorbent, *International Journal of Geomate*, **2**, 227- 234.

Janoš P., Coskun S., Pilarová V., Rejnek J., (2009), Removal of basic (Methylene Blue) and acid (Egacid Orange) dyes from waters by sorption on chemically treated wood shavings, *Bioresource Technology*, **100**, 1450-1453.

Kacurakova M., Capek P., Sasinkova V., Wellner N., Ebringerova A., (2000), FT-IR Study of plant cell wall model compounds: pectic polysaccharides and hemicelluloses, *Carbohydrate Polymers*, **43**, 195-203.

Lagergren, S., (1898), About the theory of so-called adsorption of soluble substances, *Kungliga Svenska Vetenskapsakademiens. Handlingar*, **24**, 1-39.

Langmuir I., (1918), The adsorption of gases on plane surfaces of glass, mica and platinum, *Journal of American Chemical Society*, **40**, 1362-1403.

Low M.J.D., (1960), Kinetics of chemisorption of gases on solids, *Chemical Reviews*, **60**, 267-312

Marchessault R.H., (1962), Application of Infra-red spectroscopy to cellulose and wood polysaccharides, *Pure and Applied Chemistry*, **5**, 107-129.

McKay G., Poots V.J.P., (1984), Kinetics and diffusion processes in colour removal from effluent using wood as an adsorbent, *Journal of Chemical Technology and Biotechnology*, **30**, 279-282.

Ofomaja A.E., Ho Y-H., (2007), Equilibrium sorption of anionic dye from aqueous solution by palm kernel fibre as sorbent, *Dyes and Pigments*, **74**, 60-66.

Olsson A.M., Salmen L., (2004), The association of water to cellulose and hemicellulose in paper examined by FTIR spectroscopy, *Carbohydrate Research*, **339**, 813–818.

Oz M., Lorke D.E., Petroianu G.A., (2009), Methylene blue and Alzheimer's disease, *Biochemical Pharmacology*, **78**, 927-932.

Ovchinnikov O.V., Chernykh S.V., Smirnov M.S., Alpatova D.V., Vorob'eva, R.P., Latyshev A.N., Evlev A.B., Utekhin A.N., Lukin A.N., (2007), Analysis of interaction between the organic dye methylene blue and the surface of AgCl(I) microcrystals, *Journal of Applied Spectroscopy*, **74**, 809-816.

Pastorova I., Botto R.E., Arisz P.W., Boon J.J. (1994), Cellulose char structure: a combined analytical py-GC-MS, FTIR and NMR study, *Carbohydrate Research*, **262**, 27-47.

Pavan F.A., Camacho E.S., Lima E.C., Dotto G.L., Branco V.T.A., Dias S.L.P., (2014), Formosa papaya seed powder (FPSP): preparation, characterization and application as an alternative adsorbent for the removal of crystal violet from aqueous phase, *Journal of Environmental Chemical Engineering*, **2**, 230-238.

Ponnusami V., Vikram S., Srivastava S.N., (2008), Guava (Psidiumguajava) leaf powder: Novel adsorbent for removal of methylene blue from aqueous solutions, *Journal of Hazardous Materials*, **152**, 276–286.

Redlich O., Peterson D.L., (1959), A useful adsorption isotherm, *Journal of Physical Chemistry*, **63**, 1024-1024.

Samiey B., Dargahi M.R., (2010), Kinetics and thermodynamics of adsorption of Congo red on cellulose, *Central European Journal of Chemistry*, **8**, 906–912.

Shertate R.S., Prakash T., (2014), Biotransformation of textile dyes: a bioremedial aspect of marine environment, *American Journal of Environment Science*, **10**, 489-499.

Sips R., (1948), Combined form of Langmuir and Freundlich equations, *Journal of Chemical Physics*, **16**, 490–495.

Sun R.C., Lawther J.M., Banks W.B., (1996), Fractional and structural characterization of wheat straw hemicelluloses, *Carbohydrate Polymers*, **29**, 325-331.

Temkin M.I., (1941), Adsorption equilibrium and kinetics of processes on heterogeneous surfaces and at interaction between adsorbed molecules, *Russian Journal of Physical Chemistry*, **15**, 296-332.

Tobin M.C., (1974), Theory of phase transition kinetics with growth site impingement. I. Homogeneous nucleation, *Journal of Polymer Science: Polymer Physics*, **12**, 399-406.

Toth J., (1981), A uniform interpretation of gas/solid adsorption, *Journal of Colloid and Interface Science*, **79**, 85-95.

Vadivelan V., Kumar K.V., (2005), Equilibrium, kinetics, mechanism, and process design for the sorption of methylene blue onto rice husk, *Journal of Colloid and Interface Science*, **286**, 90–100.

Vargas A.M.M., Cazetta A.L., Kunita M.H., Silva T.L., Almeida V.C., (2011), Adsorption of methylene blue on activated carbon produced from flamboyant pods (DelonixRegia): Study of adsorption isotherms and kinetic models, *Chemical Engineering Journal*, **168**, 722–730.

Vazquez G., Antorrena G., Gonzalez J., Freire S., (1997), FTIR, ^{1}H and 13C NMR characterization of acetosolv-solubilized pine and eucalyptus lignins*, Holzforschung*, **51**, 158-166.

Weber W.J., Morris J.C., (1963), Kinetics of adsorption on carbon from solution, *Journal Sanitary Engineering Division of American Society of Civil Engineering*, **89**, 31-59.

Wu F.C., Tseng R.L., Juang R.S., (2009), Characteristics of Elovich equation used for the analysis of adsorption kinetics in dye-chitosan systems, *Chemical Engineering Journal*, **150**, 366-373.

Xu A., Li X., Ye S., Yin G., Zeng Q., (2011), Catalyzed oxidative degradation of methylene blue by in situ generated cobalt (II)-bicarbonate complexes with hydrogen peroxide, *Applied Catalysis B: Environmental*, **102**, 37-43.

Zablocka-Godlewska E., Przystas W., Grabinska-Sota E., (2015), Dye decolourisation using two *Klebsiella* strains, *Water, Air, & Soil Pollution,* **226**, 2249-2263.